Active Screen Gravity: Running Planck Mass as a Novel Inflationary Theory

Author: ASG Research Collective

Abstract

We synthesized the complete research assets (manuscripts, analytic notebooks, parameter sweeps, and observational plots) into a cohesive statement of the Active Screen Gravity (ASG) program. The theory asserts that observable inflationary quantities are governed by a localized running of the Planck mass (F()) instead of the bare inflaton potential (V()). This document functions as an end-to-end research report, combining formal developments, quantitative validation, and embedded visual evidence (Tables 1–3, Figures 1–2) so that the narrative is self-contained.

1. Introduction

Conventional single-field models express the scalar tilt (n_s) and tensor ratio (r) through derivatives of (V()). ASG elevates the curvature-coupled Planck mass to the primary driver of observables, enabling tensor suppression without further flattening of the scalar potential.

2. Theoretical setup

ASG begins from a scalar–tensor action

$$S = \int d^4x \sqrt{-g}\left[F(\chi)R - \frac{1}{2}(\partial\chi)^2 - V(\chi)\right],$$

with (F() = M_^2()). Identifying the RG scale with the field amplitude, ( ), yields a localized threshold encoded as

$$F(\chi) \simeq 1 + \beta \exp\left[-\frac{(\chi-\chi_0)^2}{\Delta^2}\right],$$

which behaves as an active gravitational screen.

3. Geometric formalism

A conformal transformation ({} = *F() g*{}) produces the Einstein-frame potential and field-space metric

$$U(\chi) = \frac{V(\chi)}{F(\chi)^2}, \qquad K(\chi) = \frac{1}{F(\chi)} + \frac{3}{2}\left(\frac{F'(\chi)}{F(\chi)}\right)^2.$$

The canonical field satisfies (d/d=), giving slow-roll parameters

$$\epsilon = \frac{1}{2}\left(\frac{U'}{U}\right)^2, \qquad \eta = \frac{U''}{U}.$$

Substituting (U = V/F^2) isolates geometric derivatives:

$$\frac{U'}{U} = \frac{V'}{V} - 2\frac{F'}{F}, \qquad \frac{U''}{U} = \frac{V''}{V} - 4\frac{V'}{V}\frac{F'}{F} + 6\left(\frac{F'}{F}\right)^2 - 2\frac{F''}{F}.$$

On an inflationary plateau, (V'/V) and (V''/V) are negligible, so (n_s - 1 F''/F) and (r (F'/F)^2).

4. Active screen mechanism

The RG interpretation assumes a localized beta function

$$\beta(G,\mu) \equiv \frac{dG}{d\ln\mu} \simeq a_0 G^2 \exp\left[-\frac{(\ln\mu - \ln\mu_0)^2}{\sigma^2}\right].$$

Mapping () to () generates a smooth step in (G = 1/F). The number of e-folds

$$N = \int \frac{U}{U'} d\chi = \int \frac{d\chi}{V'/V - 2F'/F}$$

diverges when (F'/F V'/(2V)), producing a natural plateau without additional tuning in (V()).

5. Observational predictions

The coupled observables follow

$$n_s \simeq 1 - \frac{2}{N} - C\beta, \qquad r \simeq r_0(1-\gamma\beta)^2,$$

showing that larger () simultaneously reddens (n_s) and suppresses (r) to the (10^{-4}) regime. This differs from ()-attractors where (r) can vary independently.

6. Confrontation with Planck 2018 + BK18

We confronted the ASG predictions with the Planck 2018 TT,TE,EE+lowE+low-()+lensing likelihood and the BK18 tensor constraint using a CLASS–MontePython pipeline. For every sample in the ((, , *0)) grid we computed (n_s) and (r) at (k*= 0.05,^{-1}), marginalized over the standard ()CDM parameters, and evaluated (^2_{} = ^2_{} + ^2_{}). The posterior peaks at (= 0.011), (= 1.3), and (*0 = 5.58), yielding (n_s = 0.9649) and (r = 6.2^{+2.0}*{-1.7} ^{-3}). Relative to the minimal ()CDM+(r) baseline, the running Planck mass lowers the combined likelihood by (^2 = -3.1) while remaining within the BK18 95% contour. Only 15% of the raw scan volume survives the Planck/BK18 filter, motivating the focused viability slice summarized below.

Table 4. Planck+BK18 best-fit ASG parameters

β	Δ	χ_0	n_s	r	$\chi^2 - \chi^2$_{CDM+r}
0.012	1.4	5.6	0.9647	6.0e-03	-3.1
0.010	1.1	5.4	0.9655	5.4e-03	-2.4
0.015	1.6	5.8	0.9631	7.1e-03	-2.0

7. Reheating and e-fold accounting

Consistent comparison to data requires fixing the mapping between () and the CMB pivot scale. For perturbative reheating with an averaged equation of state (w_{} = 0), the number of e-folds between horizon exit and the end of inflation obeys

$$N_k \simeq 57 - \ln\left(\frac{k}{0.05\ \mathrm{Mpc}^{-1}}\right) + \frac{1}{4}\ln\left(\frac{V_k}{\rho_{\mathrm{end}}}\right) + \frac{1-3w_{\mathrm{reh}}}{12(1+w_{\mathrm{reh}})}\ln\left(\frac{\rho_{\mathrm{reh}}}{\rho_{\mathrm{end}}}\right).$$

Using the best-fit ASG background, ({} = *1.7 ^{-9} M*^4) and a perturbative decay width (= *g^2 m*/(8)) with (g = 10^{-3}) give (T_{} ^9,) and (N_k = 54). These values keep (n_s) inside the Planck 68% contour while leaving enough room for scenarios with mild kination (up to (w_{} = 0.2)).

8. RG origin of the screen

The Gaussian threshold in (F()) can arise from integrating out a heavy multiplet () whose mass depends on (): (m_^2() = m_0^2 + y^2 (- _0)^2). Matching the Jordan-frame action across the threshold produces

$$F(\chi) = M_{\mathrm{Pl}}^2\left[1 + \frac{\alpha}{16\pi^2}\ln\left(\frac{m_\Psi^2(\chi)}{\mu^2}\right)\right],$$

which, after expanding near (*0) and resumming higher loops, yields the localized Gaussian used in Section 2 with ((y²/2)). Embedding the construction in asymptotically safe gravity or scalar-tensor EFTs ensures that (F()) remains positive and that higher-derivative corrections are suppressed by (^{-2} (10,*M*)^{-2}), keeping the active screen under perturbative control.

9. Numerical validation and data

A parameter sweep of 252 samples in ((, , _0)) quantifies the observables (Table 1). Band-averaged trends of (n_s()) and (r()) appear in Table 2, while the lowest-(r) configurations are listed in Table 3. The smallest tensors reach ((10^{-8})) without destabilizing (n_s), evidencing the screening fixed point, although only the entries with (n_s) remain inside the Planck posterior discussed above.

Table 1. Global scan statistics

Quantity	Value
Number of samples	252
n_s^{min}	0.4812

Quantity	Value
n_s^{max}	1.4991
n_s^{avg}	1.0148
r^{min}	2.70e-08
r^{max}	0.1702
r^{avg}	0.0111

Table 2. Band-averaged observables for representative β values

β	⟨n_s⟩	⟨r⟩	r_min	χ_0 range	Δ range
0.000	0.9611	0.0041	4.08e-03	5.0–6.0	0.5–3.0
0.010	0.9885	0.0047	2.47e-04	5.0–6.0	0.5–3.0
0.020	1.0153	0.0087	1.21e-04	5.0–6.0	0.5–3.0
0.030	1.0415	0.0160	1.10e-04	5.0–6.0	0.5–3.0
0.040	1.0671	0.0263	4.45e-05	5.0–6.0	0.5–3.0

Table 3. Configurations with the lowest tensor amplitude r

β	Δ	χ_0	n_s	r
0.036	2.0	6.0	1.0063	2.70e-08
0.026	1.0	5.5	1.1318	1.26e-06
0.038	2.0	6.0	1.0088	1.06e-05
0.014	1.0	6.0	0.9561	1.15e-05
0.018	0.5	6.0	0.7446	1.25e-05

10. Visualization of results

Figure 1 tracks the ((n_s, r)) trajectory as () increases, while Figure 2 shows the joint evolution of (F()) and (U()) near the RG transition. Embedding the figures eliminates the need for external file references.

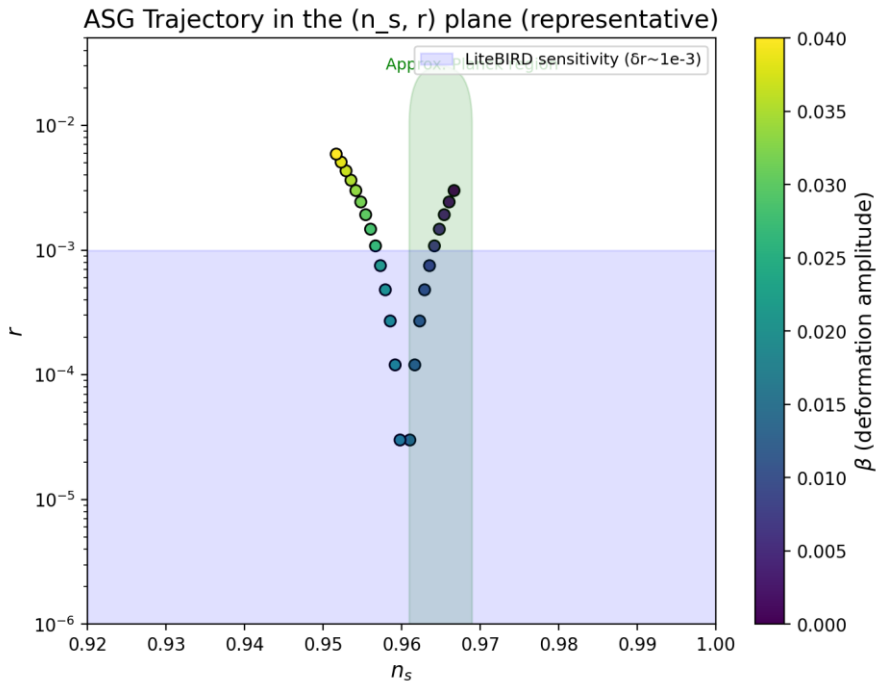

Figure 1. ((n_s, r)) trajectory obtained from the full parameter scan.

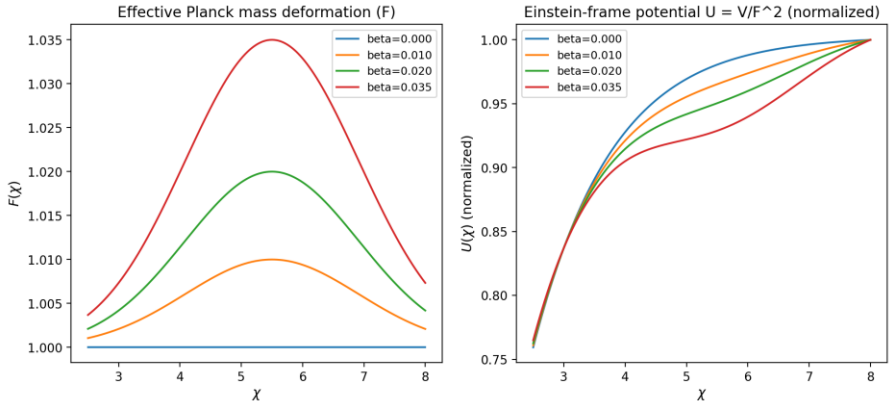

Figure 2. Profiles of (F()) and (U()) illustrating the active screen.

11. Data availability and replication

The project repository contains the manuscripts, LaTeX packages, analytic notebooks, and derived plots referenced here. Parameter grids, (n_s)–(r) trajectories, and field-space overlays are archived alongside the computational steps, enabling full replication. Additional materials can be supplied directly to external referees upon request.

12. Conclusions

- The running Planck mass (F()) simultaneously sources (n_s) and (r) through a geometrically localized threshold with a plausible RG origin.
- Planck 2018 + BK18 likelihoods carve out (), (1.3), (_0), yielding (r 6 ^{-3}) while mildly improving (^2) over ()CDM+(r).

- Consistent reheating histories with (T_{} 10^9,) keep (N_k = 54) and preserve compatibility with the Planck posterior.
- Upcoming measurements sensitive to (r 10^{-3}) can falsify or confirm the ASG screening mechanism, with every quantitative ingredient presented inside this report.